

# Velocity profiles in shear-banding wormlike micelles

Jean-Baptiste Salmon, Annie Colin, and Sébastien Manneville  
Centre de Recherche Paul Pascal, Avenue Schweitzer, 33600 Pessac, FRANCE

François Molino  
Groupe de Dynamique des Phases Condensées, Université Montpellier II,  
Place E. Bataillon, 34095 Montpellier, FRANCE

(Dated: January 11, 2022)

Using Dynamic Light Scattering in heterodyne mode, we measure velocity profiles in a much studied system of wormlike micelles (CPCI/NaSal) known to exhibit both shear-banding and stress plateau behavior. Our data provide evidence for the simplest shear-banding scenario, according to which the effective viscosity drop in the system is due to the nucleation and growth of a highly sheared band in the gap, whose thickness linearly increases with the imposed shear rate. We discuss various details of the velocity profiles in all the regions of the flow curve and emphasize on the complex, non-Newtonian nature of the flow in the highly sheared band.

PACS numbers: 83.60.-a, 83.80.Qr, 47.50.+d, 83.85.Ei

Understanding the correlation between mechanical and structural response in non-Newtonian fluids submitted to high deformation rates is crucial on both fundamental and technological grounds [1]. Among the variety of complex fluids investigated in recent years, a wide class exhibits flow-structure coupling that leads to a strong shear-thinning behavior: along the steady-state flow curve (shear stress  $\sigma$  vs. shear rate  $\dot{\gamma}$ ), a drop of up to three orders of magnitude in the effective viscosity  $\eta = \sigma/\dot{\gamma}$  is observed in a very narrow stress range leading to a stress plateau (for a review, see for instance Refs. [1, 2]). In correlation with this stress plateau, bands of different micro-structures and normal to the velocity gradient appear. Such bands correspond to a new shear-induced structure (SIS), whose low viscosity is in general supposed to be responsible for the shear-thinning. This so-called *shear-banding* behavior has been observed in both ordered mesophases (lamellar, hexagonal, cubic) [3] and transient gels [4].

A particularly well-documented example is the group of wormlike micellar systems of self-assembled surfactant molecules [5, 6]. They consist of very long cylindrical aggregates whose configurations mimic polymer solutions. However their dynamics is strongly modified by the equilibrium character of the chains, which enables them to break and recombine [7]. Generically, one starts from an isotropic viscoelastic solution of these micelles above the semidilute regime, which behaves like a Maxwell fluid at low shear rates. Upon increasing  $\dot{\gamma}$  and entering the non-linear regime, the onset of the stress plateau for a critical shear rate  $\dot{\gamma}_1$  is associated with the nucleation and growth of highly birefringent bands, suggesting strong alignment of the micelles along the velocity direction [5, 6]. As the shear rate is further increased above  $\dot{\gamma}_1$ , the new organization progressively fills the gap at almost constant stress, up to a second critical shear rate  $\dot{\gamma}_2$ . Above  $\dot{\gamma}_2$ , the system enters a second regime of apparently homogeneous

structure, with a second branch of increasing stress. The flow curve of Fig. 1 is typical of micellar systems like that investigated in the present work. Such a stress plateau has been reported for concentrations close to the equilibrium isotropic-nematic (I-N) transition, where coupling between the order parameter and the flow could explain an out-of-equilibrium phase transition to local nematic order [6, 8]. This behavior has also been observed in more dilute systems, where arguments based on instabilities in the underlying flow curve have been invoked [5, 9].

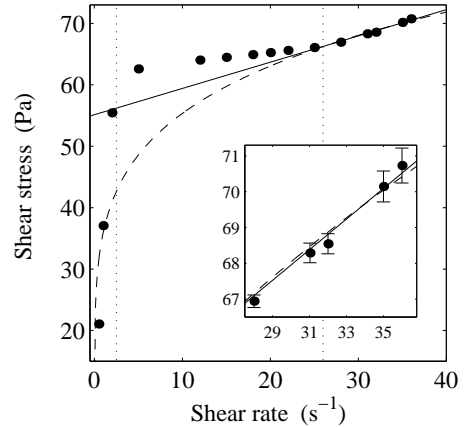


FIG. 1: Steady-state flow curve for a 6 % wt. CPCI/NaSal solution in 0.5 M brine at 21.5°C. The data were collected under controlled shear rate in a 1 mm gap Couette cell. Vertical lines indicate the limits of the banding domain. For  $\dot{\gamma} > \dot{\gamma}_2 \approx 26 \text{ s}^{-1}$ , the data were fitted by a power-law fluid  $\sigma = 35.9 \dot{\gamma}^{0.19}$  (dashed line) and by a Bingham fluid  $\sigma = 55.1 + 0.43 \dot{\gamma}$  (solid line). Inset: high shear branch; error bars account for temporal fluctuations of  $\sigma$ .

In the earliest simple pictures of the flow along the stress plateau, the system is supposed to separate into

two differently sheared bands: a weakly sheared region that flows at  $\dot{\gamma}_1$  and a highly sheared region at  $\dot{\gamma}_2$  [8, 9]. Experimentally, this very basic issue of the nature of the flow field remains rather obscure. Among previous studies, Nuclear Magnetic Resonance (NMR) imaging has proved the most successful technique to measure local velocity and/or local shear rate. Callaghan and coworkers have shown for the first time the existence of inhomogeneous velocity fields in wormlike micelles [10, 11, 12]. However, due to the limited amount of data in NRM images, no clear evidence supporting the simple shear-banding scenario has been provided. In particular, one of the most detailed NMR studies promotes a quite different dynamical description: instead of being submitted to a high shear rate, the nucleated nematic-like structure seems to undergo a zero-shear-rate plug-like flow and to move like a piece of gel, probably involving important wall slip and fracture behaviors [12]. This last observation has put the whole naive shear-thinning picture on uncertain ground.

In this Letter, we show that for the much studied wormlike micellar system CPCl/NaSal in brine and for concentrations far from the I-N transition, the simplest scenario holds. The originality of our work relies on recording both the local velocity and global rheological data in Couette geometry simultaneously along the whole flow curve. This enables to demonstrate for the first time the nucleation of a highly sheared band at a critical stress and to follow its growth from the rotor to the stator as the shear rate spans the stress plateau. We show that the width of the band grows linearly with the shear rate, in agreement with the decrease of the measured effective viscosity, and that the SIS is not Newtonian.

Our system of elongated wormlike micelles consists of a binary mixture of cetylpyridinium chloride ( $\text{CP}^+$ ,  $\text{Cl}^-$ ) and sodium salicylate ( $\text{Na}^+$ ,  $\text{Sal}^-$ ) in 0.5 M NaCl-brine. Since the pioneering work by Hoffmann and Rehage [13], this extensively studied system has been demonstrated to exhibit a stress plateau and optical birefringence shear-banding [5]. We focus on a 6 % wt. sample at 21.5°C, in the domain above the semidilute regime (0.5–5 % wt.) but far below the equilibrium I-N transition (around 20 % wt.). For the concentrations considered here, the system is known to be a perfect Maxwell fluid in the linear regime, with a typical relaxation time of about 1 s.

Rheological flow curves are measured using a standard rheometer (TA Instruments AR 1000) and transparent Couette cells of outer radius 25 mm and different gap widths  $e$  ( $e = 1$  or 3 mm). The temperature is maintained at  $21.5 \pm 0.1^\circ\text{C}$  by a water circulation around the cell. To access local velocity, we use a heterodyne Dynamic Light Scattering (DLS) technique that has been described elsewhere [14]. The measurement of the local velocity relies on performing the interference between a reference beam and light scattered from a small volume of the sample of typical size 50  $\mu\text{m}$ . The correlation func-

tion of the interference signal exhibits oscillations at the Doppler frequency  $\mathbf{q} \cdot \mathbf{v}$  where  $\mathbf{q}$  is the scattering wavevector and  $\mathbf{v}$  the local velocity. Good statistical convergence is achieved by averaging the correlation function over 3 s. Velocity profiles are measured by moving the rheometer along the velocity gradient by steps of 30  $\mu\text{m}$ . This technique enables us to obtain a complete velocity profile in about 2 min, more than 10 times faster than NMR velocity imaging. Typical uncertainties are about 5 %.

In order to enhance the scattering properties of our system, we add a small amount (1–5 % wt.) of 30 nm colloidal particles (Ludox from Aldrich). We checked that the rheological properties, particularly the plateau behavior, was not affected by the addition of those scatterers. Indeed, the small size of the scatterers compared to the typical mesh size of the micellar network in this concentration domain should lead to a negligible influence on the structural and mechanical behaviors of the sample.

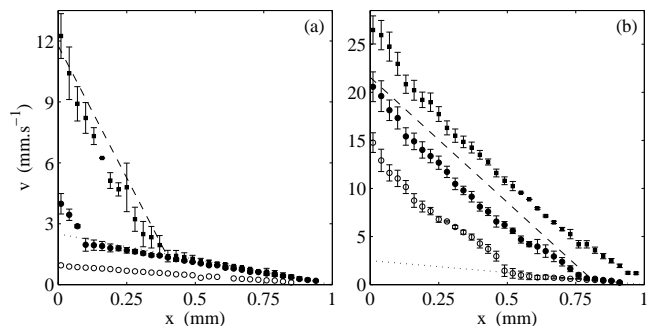


FIG. 2: Velocity profiles recorded while measuring the flow curve of Fig. 1. (a)  $\dot{\gamma} = 1$  ( $\circ$ ),  $5$  ( $\bullet$ ), and  $12$   $\text{s}^{-1}$  ( $\blacksquare$ ). (b)  $\dot{\gamma} = 15$  ( $\circ$ ),  $22$  ( $\bullet$ ), and  $28$   $\text{s}^{-1}$  ( $\blacksquare$ ). The value  $x = 0$  ( $x = 1$  resp.) corresponds to the rotor (stator resp.). The dotted line is  $v(x) = \dot{\gamma}_1(e - x)$  with  $\dot{\gamma}_1 = 2.5$   $\text{s}^{-1}$ . The dashed lines correspond to a shear rate  $\dot{\gamma}_2 = 26$   $\text{s}^{-1}$ .

Figure 1 shows the steady-state shear stress recorded in our micellar system at various imposed shear rates. This flow curve presents a stress plateau at  $\sigma \approx 65$  Pa that extends from  $\dot{\gamma}_1 \approx 2.5$   $\text{s}^{-1}$  to  $\dot{\gamma}_2 \approx 26$   $\text{s}^{-1}$  corresponding to a drop in the effective viscosity by a factor of 10. Note that for  $\dot{\gamma} > \dot{\gamma}_2$ , the stress response is no longer strictly stationary:  $\sigma$  fluctuates by about 2 % around its mean value. Finally, at  $\dot{\gamma} \approx 37$   $\text{s}^{-1}$ , the sample began to fracture so that no measurement is available at higher shear rates.

Figure 2 summarizes our main result: velocity profiles in the gap are displayed for  $\dot{\gamma}$  ranging from 1  $\text{s}^{-1}$  to 28  $\text{s}^{-1}$ . For all the shear rates in the plateau domain, the velocity profiles exhibit an unambiguous banding structure: two regions of different well-defined local shear rates coexist when  $\dot{\gamma}_1 < \dot{\gamma} < \dot{\gamma}_2$ . The highly sheared band nucleates on the inner wall of the Couette cell at

the onset of the plateau and expands as  $\dot{\gamma}$  is increased up to  $\dot{\gamma}_2$  where the band fills the whole gap. As can be seen on Fig. 2, the local shear rate in the weakly sheared region remains constant and equal to  $\dot{\gamma}_1 = 2.5 \pm 0.2 \text{ s}^{-1}$ . Moreover, although significantly curved (see below), the velocity profiles in the highly sheared region are compatible with a local shear rate of  $\dot{\gamma}_2 = 26 \pm 1 \text{ s}^{-1}$ . Note that in all our data, no noticeable wall slip was observed. Finally, these profiles easily yield the width  $h$  of the highly sheared band. Figure 3 demonstrates that  $h$  increases linearly with  $\dot{\gamma}$ . This corresponds to the simplest relation between the imposed shear rate and the two local values  $\dot{\gamma}_1$  and  $\dot{\gamma}_2$ :  $\dot{\gamma} = (1 - \alpha)\dot{\gamma}_1 + \alpha\dot{\gamma}_2$ , where  $\alpha = h/e$  increases from 0 to 1 over the plateau region.

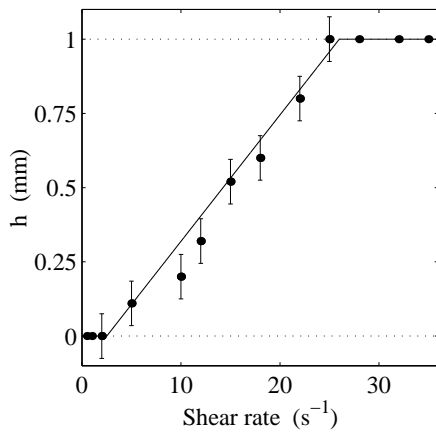


FIG. 3: Width  $h$  of the highly sheared band as a function of  $\dot{\gamma}$ . With the value  $\dot{\gamma}_1 = 2.5 \pm 0.2 \text{ s}^{-1}$  inferred from the velocity profiles of Fig. 2, a good linear approximation of  $h(\dot{\gamma})$  is obtained with  $\dot{\gamma}_2 = 26 \pm 1 \text{ s}^{-1}$  (solid line).

Beyond shear-banding evidence, the resolution of our technique enables us to analyze in more detail the flow behavior of the material in the regions below and above the plateau. In Fig. 4 are displayed two normalized velocity profiles below the plateau at  $\dot{\gamma} = 1 \text{ s}^{-1}$  and  $\dot{\gamma} = 2 \text{ s}^{-1}$  in a 3 mm gap. For  $\dot{\gamma} = 1 \text{ s}^{-1}$ , the velocity profile is very close to a straight line, consistent with the Newtonian behavior of the micellar solution at low shear rates. However, as shown in the inset of Fig. 4, our data do not exactly fall on the Newtonian velocity profile but rather present a small curvature which can be accounted for by a power-law  $\sigma \sim \dot{\gamma}^{0.7 \pm 0.1}$ . When  $\dot{\gamma} = 2 \text{ s}^{-1}$  *i.e.* just below the onset of shear-banding at  $\dot{\gamma}_1$ , the curvature is much more pronounced and the power law  $\sigma \sim \dot{\gamma}^{0.28 \pm 0.03}$  yields a perfect fit of the data. This demonstrates the existence of weak shear-thinning on the low shear branch, that sharply increases as the banding transition is approached.

Looking more closely at the velocity profiles in the plateau region, one notes that the highly sheared band displays a significant curvature even in a 1 mm gap (see

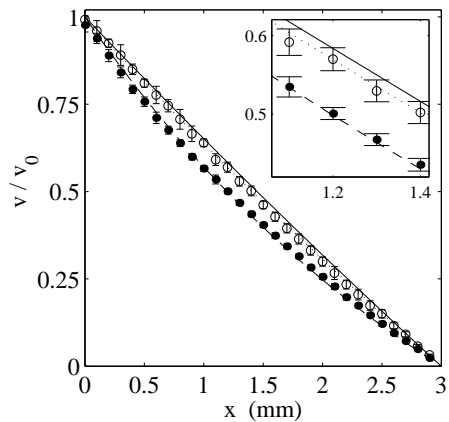


FIG. 4: Velocity profiles measured in the 3 mm gap Couette cell and rescaled by the rotor velocity  $v_0$  for two values of  $\dot{\gamma}$  below the banding transition. For  $\dot{\gamma} = 1 \text{ s}^{-1}$  ( $\circ$ ), the normalized data are well fitted by a weakly shear-thinning law  $\sigma \sim \dot{\gamma}^{0.7 \pm 0.1}$  (dotted line). For  $\dot{\gamma} = 2 \text{ s}^{-1}$  ( $\bullet$ ), a stronger shear-thinning behavior  $\sigma \sim \dot{\gamma}^{0.28 \pm 0.03}$  provides a very good fit (dashed line). The solid line is the velocity profile expected for a Newtonian fluid.

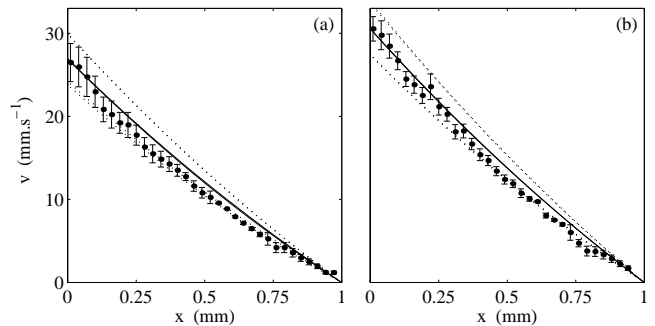


FIG. 5: Velocity profiles in the high shear branch at (a)  $\dot{\gamma} = 28 \text{ s}^{-1}$  and  $\sigma = 66.9 \text{ Pa}$  and (b)  $\dot{\gamma} = 32 \text{ s}^{-1}$  and  $\sigma = 68.5 \text{ Pa}$ . In each case, two solid lines correspond to two different but undistinguishable fits: (i) a power-law behavior  $\sigma = 35.9 \dot{\gamma}^{0.19}$  and (ii) a Bingham behavior  $\sigma = 55.1 + 0.43 \dot{\gamma}$ . The dotted lines account for a global stress fluctuation of 2 %.

Fig. 2(b)). This shows that the SIS cannot be described by a Newtonian fluid. The same observation holds for velocity profiles recorded at  $\dot{\gamma} > \dot{\gamma}_2$  where the SIS has completely invaded the gap. A precise analysis of those velocity profiles may help to understand both the global rheological measurements and the behavior of the SIS. Indeed, if one attempts to fit the flow curve of Fig. 1 for  $\dot{\gamma} > \dot{\gamma}_2$  according to a power-law  $\sigma = A\dot{\gamma}^n$ , the result is dramatically shear-thinning:  $\sigma = 35.9 \dot{\gamma}^{0.19}$  (see inset of Fig. 1). Such a shear-thinning exponent  $n$  allows us to account for the curvature of all the velocity profiles at  $\dot{\gamma} > \dot{\gamma}_2$  with a single prefactor  $A$  consistent with the rheological data (see Fig. 5 for the cases  $\dot{\gamma} = 28$  and

$32 \text{ s}^{-1}$  where the stress has been allowed to vary by 2 % according to the measured temporal fluctuations of  $\sigma$ ).

However, above  $\dot{\gamma}_2$ , other constitutive relations  $\sigma(\dot{\gamma})$  may fit the experimental data as well. For instance, a Bingham fluid  $\sigma = \sigma_0 + A\dot{\gamma}$  with  $\sigma_0 = 55.1 \text{ Pa}$  and  $A = 0.43 \text{ Pa.s}$  also closely fits both the flow curve and velocity profiles for  $\dot{\gamma} > \dot{\gamma}_2$  with a single set of parameters  $(\sigma_0, A)$  (see inset of Fig. 1 and Fig. 5). Such a Bingham behavior is suggested from the analogy with other related viscoelastic systems, whose similar nonlinear behavior has been interpreted in terms of a steady-state system of bulk fractures [4]. Here, the range of  $\dot{\gamma}$  on the high shear branch is limited to  $26\text{--}37 \text{ s}^{-1}$  so that we cannot discriminate between the two above behaviors and only further studies will help to select the correct non-Newtonian relation for the high shear branch.

Let us now further discuss our results in light of previous studies. Among the great diversity of wormlike micellar systems, a universal feature seems to emerge: the presence of a robust stress plateau associated to the growth of a SIS. However the present results and recent local NMR velocity measurements by Fischer *et al.* [12] lead to two radically different descriptions of the flow field. Ref. [12] suggests the nucleation and growth of a gel whereas our data clearly shows the coexistence of two different well-defined shear bands flowing at  $\dot{\gamma}_1$  and  $\dot{\gamma}_2$  respectively.

These important discrepancies may be explained by two different arguments. First, the distance to the I-N transition is drastically different in the systems under study. Indeed, Fischer *et al.* used a CTAB/D<sub>2</sub>O system at a surfactant concentration of 20 % wt. very close to the I-N transition ( $\approx 21 \text{ % wt.}$  at the working temperature). In our case (CPCl/NaSal in brine), the surfactant concentration of 6 % wt. was much more distant from the I-N transition. Second, significant temporal fluctuations of the flow field are mentioned in both the present work and Refs. [11, 12]. If the flow of the SIS is time-dependent, we think that the data analysis in the two techniques may be affected in different ways. The temporal resolution of our heterodyne DLS setup provides an accurate value of the local velocity averaged over a few seconds. With NMR imaging, a broad velocity distribution is reported in the SIS, sometimes showing several peaks. We believe that this rich spectral content may complicate the interpretation of the average NMR data.

Another important open issue concerns the very nature of the SIS and its rheological behavior. As far as the structure is concerned, birefringence appears as a robust experimental fact [5, 6]. However, the correlation between birefringence and local nematic order is only confirmed for systems close to the I-N transition [11]. This points to possible differences between shear-induced structures far from and close to this equilibrium transi-

tion. As for the behavior under shear, flow instabilities in the SIS at high shear rates leads to fracture and ejection of the sample from the rheometer [5, 9]. We believe that the non-Newtonian features of the SIS revealed in this Letter may play an important role in such instabilities. Indeed temporal fluctuations of the stress and of the birefringent bands seem to suggest intermittent and localized fracture-like flow events, yet not directly observed so far.

Although separate studies of rheology, birefringence, and more recently NMR velocity profiles, have been performed, a complete picture of the nonlinear rheology of wormlike micelles remained rather elusive in the literature due to the lack of experimental data. Coupled with optical birefringence and rheological measurements, our heterodyne DLS setup appears as a well-suited tool to provide the missing information on this much studied problem.

The authors are grateful to the “Cellule Instrumentation” at CRPP for building the experimental setup. We also thank J.-F. Berret, C. Gay, and P. Olmsted for fruitful discussions.

- 
- [1] R. G. Larson, *The Structure and Rheology of Complex Fluids* (Oxford University Press, 1999).
  - [2] M. E. Cates and M. R. Evans, eds., *Soft and Fragile Matter: Non Equilibrium Dynamics Metastability and Flow* (Institute of Physics Publishing (Bristol), 2000).
  - [3] D. Roux, F. Nallet, and O. Diat, *Europhys. Lett.* **24**, 53 (1993); L. Ramos, *Phys. Rev. E* **64**, 061502 (2001); E. Eiser, F. Molino, and G. Porte, *Phys. Rev. E* **61**, 6759 (2000).
  - [4] F. Molino, J. Appell, M. Filali, E. Michel, G. Porte, S. Mora, and E. Sunyer, *J. Phys.: Condens. Matter* **12**, A491 (2000).
  - [5] J.-F. Berret, D. C. Roux, and G. Porte, *J. Phys. II* **4**, 1261 (1994); J.-F. Berret, G. Porte, and J.-P. Decruppe, *Phys. Rev. E* **55**, 1668 (1997).
  - [6] V. Schmitt, F. Lequeux, A. Pousse, and D. Roux, *Langmuir* **10**, 955 (1994).
  - [7] M. E. Cates, *Macromolecules* **20**, 2289 (1987).
  - [8] P. D. Olmsted and C.-Y. D. Lu, *Phys. Rev. E* **56**, 55 (1997).
  - [9] A. Spenley, M. E. Cates, and T. C. B. McLeish, *Phys. Rev. Lett.* **71**, 939 (1993).
  - [10] R. W. Mair and P. T. Callaghan, *Europhys. Lett.* **36**, 719 (1996).
  - [11] M. M. Britton and P. T. Callaghan, *Phys. Rev. Lett.* **78**, 4930 (1997); *Eur. Phys. J. B* **7**, 237 (1999).
  - [12] E. Fischer and P. T. Callaghan, *Phys. Rev. E* **64**, 011501 (2001).
  - [13] H. Rehage and H. Hoffmann, *Mol. Phys.* **74**, 933 (1991).
  - [14] J.-B. Salmon, S. Manneville, A. Colin, and B. Pouligny (2002), E-print cond-mat/0211013 submitted to *Eur. Phys. J. AP*.